

Received July 10, 2021, accepted July 23, 2021, date of publication August 3, 2021, date of current version August 10, 2021.

Digital Object Identifier 10.1109/ACCESS.2021.3102020

Research on the Processing of Coal Mine Water Source Data by Optimizing BP Neural Network Algorithm With Sparrow Search Algorithm

PENGCHENG YAN^{1,2}, SONGHANG SHANG², CHAOYIN ZHANG², NINI YIN¹,
XIAOFEI ZHANG², GAOKUN YANG², ZHUANG ZHANG², AND QUANSHENG SUN²

¹State Key Laboratory of Mining Response and Disaster Prevention and Control in Deep Coal Mine, Anhui University of Science and Technology, Huainan 232001, China

²College of Electrical and Information Engineering, Anhui University of Science and Technology, Huainan, Anhui 232001, China

Corresponding author: Songhang Shang (13329078709@163.com)

This work was supported in part by the National Key Research and Development Program of China under Grant 2018YFC0604503, in part by Anhui Province Natural Science Foundation for Youths under Grant 1808085QE157, in part by Anhui Provincial Postdoctoral Research Funding Programs under Grant 2019B350, and in part by China National Coal Association 2018 Science and Technology Research Guiding Plan Program under Grant MTKJ2018-258.

ABSTRACT Coal mine safety is crucial to the healthy and sustainable development of the coal industry, and coal mine flood is a major hidden danger of coal mine accidents. Therefore, the processing of coal mine water source data is of great significance to prevent mine water inrush accidents. In this experiment, the water source data were obtained by laser induced fluorescence technology with the assistance of laser. The water sample data information was preprocessed by standard normal variable transformation (SNV) and multiple scattering correction (MSC), and then the principal component analysis (PCA) was used to reduce the dimension of the data and ensure the information characteristics of the original data unchanged. In order to identify the water inrush type of coal mine water source, the sparrow search algorithm (SSA) is used to optimize the BP neural network in this study. This is because the SSA algorithm has the advantages of strong optimization ability and fast convergence rate compared with particle swarm optimization (PSO) and other optimization algorithms. Experiments show that under the premise of SNV pretreatment, the R^2 of SSA-BP model is infinitely close to 1, MRE is 0.0017, RMSE is 0.0001, the R^2 of PSO-BP model is 0.9995, MRE is 0.0026, RMSE is 0.0019, the R^2 of BP model is 0.9983, MRE is 0.0140, RMSE is 0.0075. Therefore, SSA-BP model is more suitable for the classification of coal mine water sources.

INDEX TERMS Laser induced fluorescence technique, pretreatment, sparrow search algorithm.

I. INTRODUCTION

Coal occupies an important social position in the development of national economy [1]–[4], according to «BP2035 Energy Outlook» released by BP Energy Company, China's coal consumption will remain stable for a longer period of time, peaking in 2025 and then remain stable for the next decade. It can be seen that the coal industry has made great contributions to China's economic development [5]–[7], but coal mining will encounter various safety problems in safety production and construction [8]–[11]. According to the coal mine safety data released by the accident inquiry system of the National Mine Safety Administration, only

The associate editor coordinating the review of this manuscript and approving it for publication was Sabah Mohammed¹.

in 2020, 122 accidents occurred in coal mining enterprises and 225 people died. So it is very important to reduce the occurrence of mine accidents for people's life safety and national production and construction [12], [13].

Mine accidents mainly include gas accidents, roof accidents, mechanical and electrical accidents, blasting accidents, flood accidents, fire accidents, transportation accidents, and other accidents [14]–[20], among which mine water disaster accidents are the most serious. Mine water disaster accidents generally occur at the mining working face. When the coal mining face encounters underground rivers or aquifers with strong water-richness, large-scale water gushing will occur and enter the coal mining roadway. Once the mine water inrush accident occurs, the coal mining face will be submerged lightly and the coal mining tools will be destroyed,

which will lead to mine damage and cause significant loss of personnel and property. Therefore, it is urgent to prevent and control mine water disasters, and rapid headstream recognition of mine water-bursting is a powerful tool to solve mine water disasters [21].

Mine water sources are mainly divided into four categories: atmospheric precipitation, surface water, groundwater, and old goaf water [22]–[25]. Atmospheric precipitation is the main source of groundwater in mines; Surface water mainly refers to different types of water, such as streams, rivers, lakes and artificial reservoirs; Groundwater is subdivided into karst groundwater, fissure groundwater, and pore groundwater according to the characteristics of aquifer; The old goaf water refers to the water body in the ancient kiln or small kiln where the mining location and scope are not clear in the process of mining.

The traditional method of judging the type of coal mine water source is mainly using the method of hydrochemistry [26]. This is because in the process of the formation of coal mine water source, the lithosphere, hydrosphere, atmosphere, biosphere and the water body contained in the formation are all kinds of physical and chemical effects, which also causes the continuous transformation of the chemical composition of groundwater. Hydrochemical identification of coal mine water types which is mainly based on the use of groundwater containing different ion concentrations of water classification. For example, the representative ion method uses the particle concentration of 7 elements in the water source to classify the mine water source through classical methods such as Pipertu and Shukalev, and then compares the water quality of the inflow water and the water quality of the classified aquifer to identify the water source type [27], [28]. Other widely used methods include isotope method, trace element method, radioactive element method, water temperature and water level method, and GIS method [15], [29]–[33]. However, due to the particularity of the water chemistry method experiment, the operation is complex and the data is unstable, so it is urgent to find a new method for the classification and prediction of coal mine water sources.

Due to the rapid development of photoelectric technology, spectral analysis has also made great progress in theory and practice. A large number of theories and methods have sprung up, and many well-known working teams have emerged. With the progress of spectral analysis technology, laser-induced fluorescence (LIF) technology has also been successfully applied and developed in many fields. In [34], Wang *et al.* of Tsinghua University proved that the laser-induced fluorescence technology was an advanced test technology for detecting the flow-mixing behavior of chemical processes in a variety of experimental methods for studying the mixing process. The test principle and implementation of this technology were introduced in detail, and the research progress of this technology in visual liquid mixing process and reaction flow mixing process was discussed. In [35], Li *et al.* of Beijing Institute of Technology of Technology carried out quantitative analysis of doping in virgin olive oil by laser

induced fluorescence technique. In [36], in order to detect petroleum pollutants in soil, Zuo *et al.* of University of Science and Technology of China constructed a laser-induced fluorescence experimental system, and made a detailed study on the overlapping characteristics of fluorescence signals of mobile oil and diesel mixtures in soil by iterative approximation algorithm.

The application of laser technology has gone deep into all aspects of industrial production, which has the characteristics of fast and accurate. Therefore, this experiment proposed for the first time the laser-induced fluorescence technology as the key technology for the identification of coal mine water sources. The fluorescence spectrum information of coal mine water sources was collected according to the LIF technology, and then the data were processed by the neural network to make classification and prediction of coal mine water sources. The main purpose of this experiment is to use the spectral information of mine water source to reduce the dimension of the spectral information of different water samples and extract the characteristic factors through a series of pretreatment methods. The spectral characteristics of coal mine water sources are obtained and the principal component analysis is carried out. At the same time, a variety of identification models of mine water sources are established and the prediction and classification are carried out.

In the whole article, this study uses BP neural network algorithm, but the classification accuracy of mine water source by using BP neural network alone is not high, so the optimization algorithm is needed. Common optimization algorithms include PSO algorithm and genetic algorithm. In recent years, monarch butterfly optimization (MBO), slime mould algorithm (SMA), moth search algorithm (MSA), hunger games search (HGS), Runge Kutta method (RUN), and Harris hawks optimization (HHO) are all optimization algorithms and have received extensive attention [37]–[42].

MBO algorithm is a swarm intelligence optimization algorithm inspired by the migration behavior of the monarch butterfly in the United States. The migration operator and the adjustment operator can determine the search direction of the monarch butterfly at the same time. Therefore, MBO is suitable for parallel processing be weighed between intensification and diversification. However, MBO has weak global search ability and it is prone to reduce population diversity in the migration process. The inspiration of SMA comes from the diffusion and foraging behavior of slime mould. The weight index is used to simulate the three correlations between the morphological changes and contraction modes of myxobacteria venous tubes. The moth search algorithm is a meta-heuristic optimization algorithm based on the phototaxis of moths and Levy flights of moths. HGS is an optimization algorithm formed by hunger desires and resulting animal behavior choices, it uses adaptive weight updates to ensure higher survival and access to food to adapt to evolution. Runge Kutta method is used to explore promising regions and to move towards global optimal solution in feature space. HHO is an intelligent optimization algorithm to simulate the

predatory behavior of Harris Hawks. It is mainly composed of three parts: the search stage, the transformation of search and development, and the development stage. The current position of the prey is obtained by constantly updating the fitness value of the prey.

The focus of this paper is to use BP neural network and its optimization algorithm to realize the classification of mine water source. The main architecture includes the experimental part, including the preparation of the experimental object and the construction of the laser induced fluorescence device. Then the particle swarm optimization BP (PSO-BP) network prediction classification model, the establishment of SSA-BP model, the comparison of the results of each model and the analysis are more suitable for the classification and recognition model of mine water inrush source. At the end of the article is a summary of the whole article. The algorithm models involved in this paper are all operated in the MATLAB R2016a working environment during the establishment process.

II. EXPERIMENT PART

The purpose of the experiment is to predict and classify mine water sources based on the identification mechanism of laser induced fluorescence spectrum characteristics of coal mine water sources. Firstly, water samples from different regions were collected, and water molecules were excited to quantum state by high-intensity laser. At this time, the spectral data were obtained by immersion fluorescent probes. Secondly, the complex data were preprocessed by PCA dimension reduction. Finally, the spectral characteristics of the extracted data were modeled and predicted by neural network. The specific process is shown in Fig. 1.

In order to select the optimal model for mine water source classification, MSC and SNV preprocessing methods were used to reduce the calculation amount of data before dimension reduction. PSO and SSA were used to optimize the BP neural network, and the optimal model was selected through the evaluation index of different models.

A. MATERIAL PREPARATION

Because the water source types of coal mine are mostly old goaf water, so the experimental object selects the karst water and old goaf water collected in Xinhuangzi Coal Mine. In the experimental preparation stage, karst water and old goaf water were mixed, and the mixing ratio was (1~10): 10, 10: (1~10), a total of 20 kinds of mixed water samples. The water samples to be measured are two kinds of pure water samples of karst water and old goaf water and mixed water samples mixed together in different mixing ratios. The mixing ratios were randomly selected from 20 ratios, which were 10: 3, 10: 6, 10: 10, 6: 10, and 3: 10. Therefore, the number of water samples was 7, and 30 copies were taken from each water sample, that is, the total number of experimental samples was 210, which were stored in dark.

In the process of PCA dimensionality reduction and the establishment of BP algorithm and its optimization algorithm

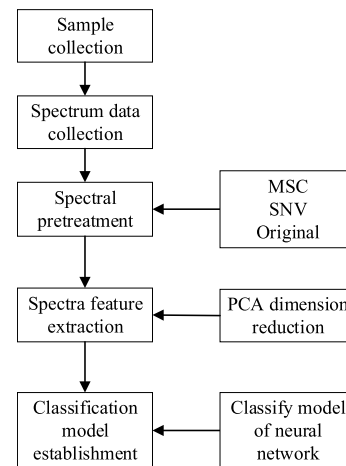


FIGURE 1. Flow chart of mine water source classification model.

model, the training set takes the first 20 copies from 30 samples of each water sample, and the last 10 copies as the test set. Since there are seven kinds of water samples, there are 140 training sets and 70 test sets.

B. SPECTRAL ACQUISITION

In the spectral acquisition part, a laser-induced fluorescence experimental device is built with laser, optical fiber, micro fluorescence probe and spectrometer. The laser is supplied by +12V DC power, the power can be adjusted continuously in 90-130mw.

The sample to be tested was incident to the laser excitation spectrum at 405 nm. The laser power was set to be 100 mw, and the integration time was set to be 1/1000 nm. The immersion fluorescent probe (GUANGZHOU BIAOQI OPTOELECTRONICS) was directly used to put it into the water to be tested to excite the fluorescence. The appropriate band of fluorescence was obtained by the wavelength selection element, and the spectral information to be tested was received by the spectral detector. The spectrometer is produced by Ocean Optics USB2000+ spectrometer, which is supplied by 5V DC power. Spectral acquisition and reception are recorded by Ocean View software, and the whole experiment process is carried out in the darkroom. The experimental device for laser-induced fluorescence detection of water source is shown in Fig. 2.

C. SPECTRAL PRETREATMENT

During the experiment, because the original fluorescence spectrum is affected by instrument noise and power fluctuation, there will be a large number of fluctuation “burrs” on the spectrum, and the interference information collected will affect the accuracy of the experimental results. Therefore, the pretreatment is used to quantitatively and qualitatively analyze the spectral data to improve the accuracy of the experiment.

The original spectra of samples collected by Ocean View software are shown in Fig 3. The detection range of light

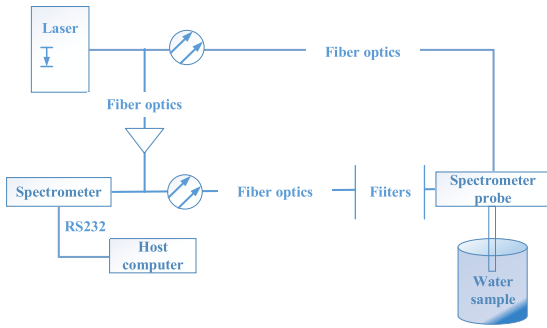


FIGURE 2. Laser induced fluorescence experimental device.

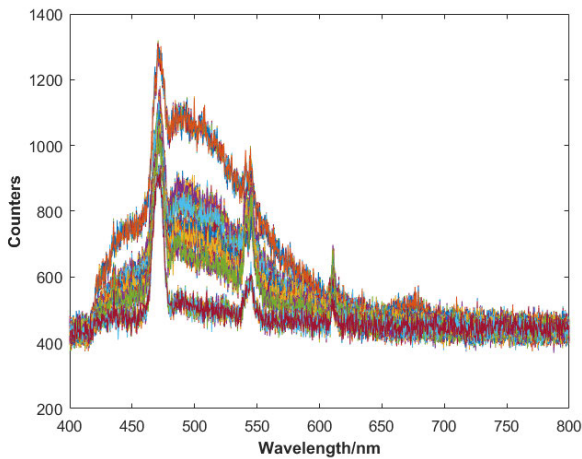


FIGURE 3. Original spectra.

wavelength is 400 – 800 nm, and the variation range of spectrum is mainly concentrated in the light wavelength of 400 – 700 nm. The spectral intensity between 700 – 800 nm tends to be stable.

1) MULTIPLE SCATTERING CORRECTION MSC

The purpose of multiple scattering correction is to eliminate the influence of optical path change or uneven distribution of the material to be measured on the infrared diffuse reflectance spectrum. MSC algorithm is mainly through the spectral information of a set of experimental samples, which is based on statistical methods to correct the linear changes caused by scattering, eliminate the baseline shift and drift between samples, and enhance spectral specificity [43].

The pretreatment steps of MSC for the original spectrum collected in the experiment are as follows: Firstly, the average spectrum was selected as the standard spectrum. Then the intercept b_i and coefficient k_i are obtained by linear regression with original spectrum and standard spectrum. Finally, each sample is corrected.

$$\begin{cases} \bar{A} = \frac{1}{n} \sum_{i=1}^n A_i \\ A_i = k_i \bar{A} + b_i \\ A_{i(MSC)} = \frac{A_i - b_i}{k_i} \end{cases} \quad (1)$$

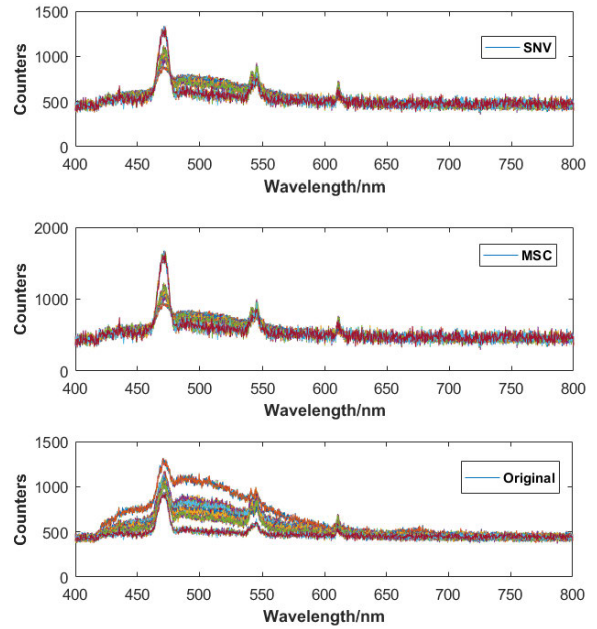


FIGURE 4. Pretreatment images include three pretreatment methods, including SNV, MSC, and Original.

where \bar{A} is the standard spectral data, A_i represents the i^{th} line of spectral data matrix A . $A_{i(MSC)}$ is the spectroscopic data after calibration

2) STANDARD NORMAL VARIABLE TRANSFORM SNV

The pretreatment of spectrum by SNV algorithm is mainly to calculate the rows of spectral array, that is, the pretreatment object is a certain spectral information. This preprocessing algorithm is mainly to eliminate the influence of scattering and diffuse reflection caused by the surface particles and non-uniformity of the measured object, such as optical path change, surface scattering and solid particle size, etc. The spectra which need SNV pretreatment are calculated by formula (2).

$$A_{i,SNV} = \frac{A_{i,k} - \bar{A}}{\sqrt{\frac{\sum_{k=i}^m (A_{i,k} - \bar{A})^2}{m-1}}} \quad (2)$$

where $A_{i,SNV}$ is the transformed spectrum, m is the number of wavelength points, $k = 1, 2, \dots, m$.

The pretreatment images are shown in Fig. 4.

D. PCA DIMENSION REDUCTION

Principal component analysis (PCA) is mainly used for dimension reduction of data, and the main component elements are analyzed from the multivariate factors in a data set, so as to reveal the characteristics of the data set according to these main component elements [44]. The purpose of PCA is to map high dimensional data into low dimensional space, retain the original features of the data set to the greatest extent, and reduce the computational complexity and

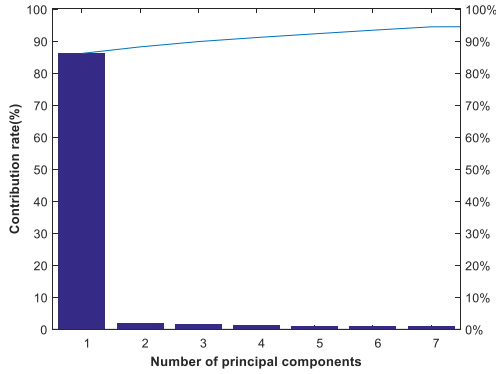


FIGURE 5. Principal component contribution rate.

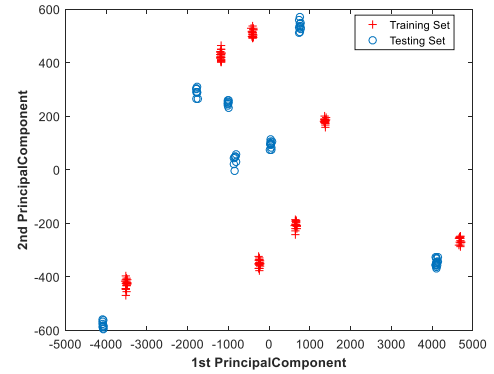


FIGURE 7. Score distribution diagram.

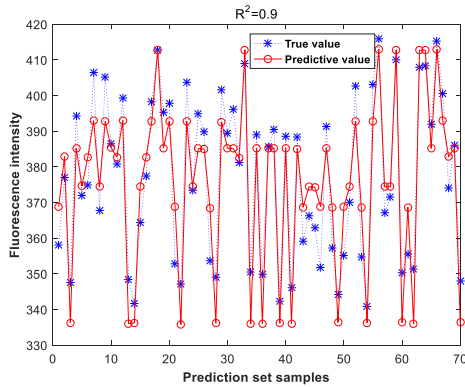


FIGURE 6. Comparison of test set prediction results.

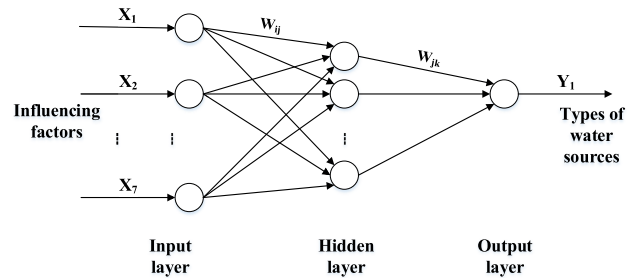


FIGURE 8. BP neural network topology.

complexity of the later modeling. The general steps of PCA are as follows:

- 1) The data set is converted into a matrix $X_{n \times m}$, explaining the variables and making zero mean work.
- 2) Solving the covariance matrix of matrix X .
- 3) Calculating the principal component of the data. Principal component is the eigenvector corresponding to eigenvalues.
- 4) Mapping data to principal components.

PCA dimensionality reduction is performed on 210 selected samples. The number of principal components is 7, and the contribution rate of principal components is shown in Fig. 5. When the principal component is 1, the contribution rate reaches 94%.

The clustering effect of water samples is obvious when the first principal component is compared with the second principal component, and the determination coefficient of the model reaches 0.9 in Fig. 6. The score distribution is shown in Fig. 7.

III. PSO-BP NEURAL NETWORK CLASSIFICATION MODEL

A. BP NEURAL NETWORK

BP neural network is a multilayer feedforward neural network, whose main feature is forward transfer of signal [45], [46], and its topological structure is shown in Fig. 8.

According to the topological structure of neural network, X_1, X_2, \dots, X_7 are the input value of the network, Y_1 is the output value of the network, BP neural network reflects the function mapping relationship between independent variables and dependent variables. In this experiment, the input value of the network is the factor affecting the type of mine water source, and the output value is the type of mine water source.

The precondition of BP neural network to complete the prediction classification is to train the network, and make it have associative memory and prediction ability through training, so as to realize the prediction classification of coal mine water source by network.

B. NETWORK PARAMETER SELECTION

The number of hidden layer nodes h in BP neural network is obtained by formula 3.

$$\begin{cases} h < n - 1 \\ h < \sqrt{(m + n)} + a \\ h = \log_2 n \end{cases} \quad (3)$$

where h is the number of hidden layer nodes, m is the number of output layer nodes, n is the number of input layer nodes, $a = 1, 2, \dots, 10$, which is the adjustment constant between hidden layers.

Different values of a will affect the training error of the neural network. On the premise that the number of hidden layer nodes can be arbitrarily adjusted, the number of hidden layer nodes is set to 6–15. The neural network model is established and the network training is carried out, and the

TABLE 1. The training error corresponding to the number of different hidden layer nodes.

The Number of Hidden Layer Nodes	6	7	8	9	10	11	12	13	14	15
Training Error	0.274	0.089	0.039	0.039	0.039	0.037	0.661	0.035	0.039	0.037

training errors of different hidden layer nodes are obtained, as shown in Table 1.

When the number of hidden layer nodes is 13, the training error is the smallest, so the number of hidden layer nodes in the BP neural network prediction experiment of mine water source classification is 13. Other training parameters such as training times set to 1000, training target minimum error 0.001, learning rate set to 0.01.

C. PSO ALGORITHM OPTIMIZATION MODEL

PSO algorithm, particle swarm optimization algorithm, which is derived from the study of bird predation. This algorithm is the simplest way to each bird to find food by searching the surrounding area of the bird closest to the object. PSO algorithm is inspired by this biological feature and used to solve optimization problems [47]–[49]. The PSO algorithm uses position, velocity and fitness value to represent the particle characteristics, and determines the optimal position by tracking individual extremum P_{best} and group extremum G_{best} . Suppose there is a D -dimensional target search space, there is a population of n particles $Z = (X_1, X_2, \dots, X_n)$, there is a i particle in the population Z can be expressed as a D -dimensional vector $X_i = [x_{i1}, x_{i2}, \dots, x_{iD}]^T$, which represents a potential solution vector of a problem in D -dimensional space, and the fitness value of each X_i particle position is determined according to the objective function. The velocity of the i th particle is $V_i = [V_{i1}, V_{i2}, \dots, V_{iD}]^T$, the individual extreme value is $P_i = [P_{i1}, P_{i2}, \dots, P_{iD}]^T$, and the population extreme value is $P_g = [P_{g1}, P_{g2}, \dots, P_{gD}]^T$.

During the iteration, the velocity and position of particles are updated by the following formula.

$$\begin{cases} V_{id}^{k+1} = wV_{id}^k + c_1r_1(P_{id}^k - X_{id}^k) \\ \quad + c_2r_2(P_{gd}^k - X_{id}^k) \\ X_{id}^{k+1} = X_{id}^k + V_{id}^{k+1} \end{cases} \quad (4)$$

where w is inertia weight, $d = 1, 2, \dots, D, i = 1, 2, \dots, n, k$ is the current iteration number, V_{id} is particle velocity, c_1 and c_2 are acceleration constants, r_1 and r_2 are random numbers between $[0, 1]$.

D. ESTABLISHMENT OF PSO-BP CLASSIFICATION MODEL

The main parameters of PSO-BP classification model such as acceleration factors c_1 and c_2 are 1.49445, the number of evolution is set to 20, and the population size is set to 30. The basic steps of PSO-BP prediction model are as follows [50]–[53].

- 1) The BP neural network selects the single hidden layer network topology. The influencing factors of mine water source types are used as the network input, and

the water source types are the network output. The optimal number of hidden layer nodes is determined according to the adjustment constant a .

- 2) The particle and velocity of PSO algorithm are initialized to determine the particle population n , particle velocity v and population dimension D .
- 3) The data set after dimension reduction and preprocessing is divided into training set and test set, and imported into PSO-BP classification model.
- 4) Running the PSO-BP model, calculate the particle fitness value according to the fitness function. The individual position is updated by tracking the individual P_{best} and the group extreme G_{best} , and the convergence precision is set to make G_{best} approach this precision continuously.
- 5) The G_{best} within the range of convergence accuracy is assigned to the BP neural network as the weight and threshold of the network.
- 6) According to the neural network trained by the training set, use this as a standard to predict and process the test set and test the results.

IV. ESTABLISHMENT OF SSA-BP MODEL

Sparrow search algorithm (SSA) is a bionic intelligent optimization algorithm proposed by Xue and Shen. This algorithm proposes an intelligent optimization classification algorithm based on the predation and anti-predation behaviors of sparrows during foraging [54]–[57]. In this foraging process, sparrows are divided into discoverers and adders. The discoverer has a high fitness value and is responsible for searching the optimal region, providing foraging regions and directions for all adders. In order to improve their predation rate, some adders will monitor the discoverers and predators. On the one hand, once the discoverers find areas with rich food, the adders will immediately foraging or competing for food resources around them. On the other hand, when the population is threatened by predators, they will issue early warning information to make the population move to the safe area [58]. Assuming that there are N sparrows in a D -dimensional space, the position of each sparrow is $X = [x_1, x_2, \dots, x_D]$, and the fitness value $f = f(x_1, x_2, \dots, x_D)$. The algorithm mainly includes the update of three parts of the formula.

Firstly, the location update formula of the discoverer is as follows:

$$\alpha X_{m,d}^{t+1} = \begin{cases} X_{m,d}^t \cdot \exp\left(-\frac{m}{B_{max}}\right), & R_2 < ST \\ X_{m,d}^t + Q \cdot L, & R_2 \geq ST \end{cases} \quad (5)$$

where $X_{m,d}$ represents the position information of the m^{th} sparrow population in the d^{th} dimension, $t + 1$ is the current iteration number, which belongs to the uniform random number between (0,1), α is a uniform random number between (0,1], B_{\max} is the limit of iteration number, Q is a random number of standard normal distribution, L is a matrix of $1 \times D$ and all elements are 1, R_2 is the uniform random number between [0,1], which indicates the early warning value of the sparrow population, and ST is the safe value of the safe position of the population of [0.5,1].

When $R_2 < ST$, the warning value is less than the safety value, indicating that the population does not find predators and is in a safe position to search for food. At this time, the discoverer can expand the range of food search and obtain more abundant food supplies. When $R_2 \geq ST$, the warning value is greater than the safety value, which means that some sparrows in the population find predators, send dangerous signals to the population, stop foraging, and make anti-predation behavior, close to the safe area.

Secondly, except for the discoverer, the other sparrows are all adders, and the position is updated. The update formula is as follows.

$$X_{m,d}^{t+1} = \begin{cases} Q \cdot \exp\left(\frac{X_{\text{worst}}^t - X_{m,d}^t}{m^2}\right), & m > \frac{n}{2} \\ X_{\text{best}}^{t+1} + |X_{m,d}^t - X_{\text{best}}^{t+1}| \cdot A^+ \cdot L, & m \leq \frac{n}{2} \end{cases} \quad (6)$$

where X_{best}^{t+1} represents the optimal position of the population when the number of iterations is $t + 1$, X_{worst}^t is the worst position when the number of iterations is t , and A^+ is the $1 \times d$ matrix with all elements of 1 or -1 , and satisfies $A^+ = A^T \cdot (AA^T)^{-1}$. When $m > n/2$ indicates that the m^{th} sparrow with low fitness does not obtain food, and it is in a state of hunger. It is necessary to go to the safe area to find food improve the predation rate, and supplement energy. When $m \leq n/2$, the m^{th} adder is foraging in the optimal area.

Finally, some sparrows will be responsible for reconnaissance and early warning when the population foraging. Once the natural enemy is found, all sparrows stop foraging and transfer to a safe position. The number of early warning sparrows generally accounts for 10% - 20% of the total population, and their locations are updated as follows.

$$X_{m,d}^{t+1} = \begin{cases} X_{\text{best}}^t + \beta (X_{m,d}^t - X_{\text{best}}^t), & f_m \neq f_g \\ X_{m,d}^t + K \cdot \left(\frac{X_{m,d}^t - X_{\text{worst}}^t}{|f_m - f_w| + e}\right), & f_m = f_g \end{cases} \quad (7)$$

where K is a uniform random number in the range of $[-1, 1]$, f_m is the current fitness value, f_w is the global minimum fitness value, and f_g is the global optimal fitness value. The reason why e exists is to prevent the denominator from being zero. When $f_m \neq f_g$, indicating that the sparrow in the edge of the population, vulnerable to the threat of natural enemies. When $f_m = f_g$, it means that the sparrows in the center of the population are also at risk. In order to avoid being preyed, we should try to close to other sparrows, adjust

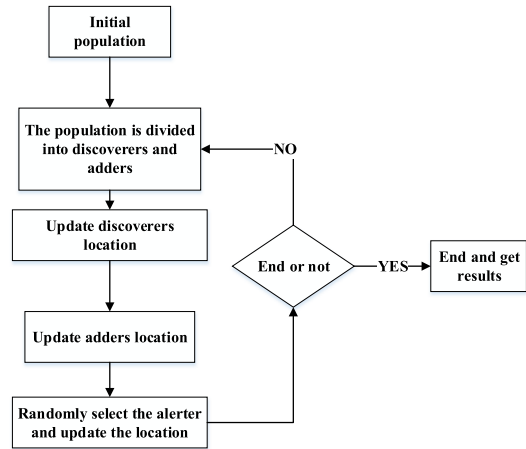


FIGURE 9. Flow chart of SSA-BP algorithm.

the search strategy, β is the step size control coefficient, and it is a normal distribution random number with mean value of 0 and variance of 1.

The flow chart of SSA optimizing BP neural network is shown in Fig. 9.

The purpose of using SSA to optimize BP neural network is to obtain the optimal weight, threshold and the optimal fitness value. SSA-BP model training parameters such as the number of evolution is 20, population size 30. The complexity of this model is how to determine the optimal proportion of discoverers. The different number of discoverers will lead to unstable classification results. Therefore, in this design process, we constantly change the proportion of discoverers and find that when it is 0.2, the classification accuracy is the highest.

V. MODEL RESULTS AND ANALYSIS

Four evaluation indexes of the model are introduced before analyzing the results of each model, which are the coefficient of determination R^2 , the mean relative error (MRE), the root mean square error (RMSE), and the absolute error.

The coefficient of determination R^2 is the square of the correlation coefficient, also known as the goodness of fit [59], [60], which can explain the reason why the dependent variable changes due to the change of independent variables. The size of the coefficient of determination determines the degree of correlation. When R^2 is infinitely close to 1, it indicates that the degree of correlation is higher; when R^2 is close to 0, it indicates that the degree of correlation is lower. Therefore, the larger the coefficient of determination, the higher the degree of explanation of the independent variable to the part of the dependent variable, and the smaller the coefficient of determination. The lower the degree of correlation, the lower the percentage of the change caused by the independent variable in the total change. The calculation formula of R^2 is as follows.

$$R^2 = \frac{\sum_i (f_i - \bar{y})^2}{\sum_i (y_i - \bar{y})^2} \quad (8)$$

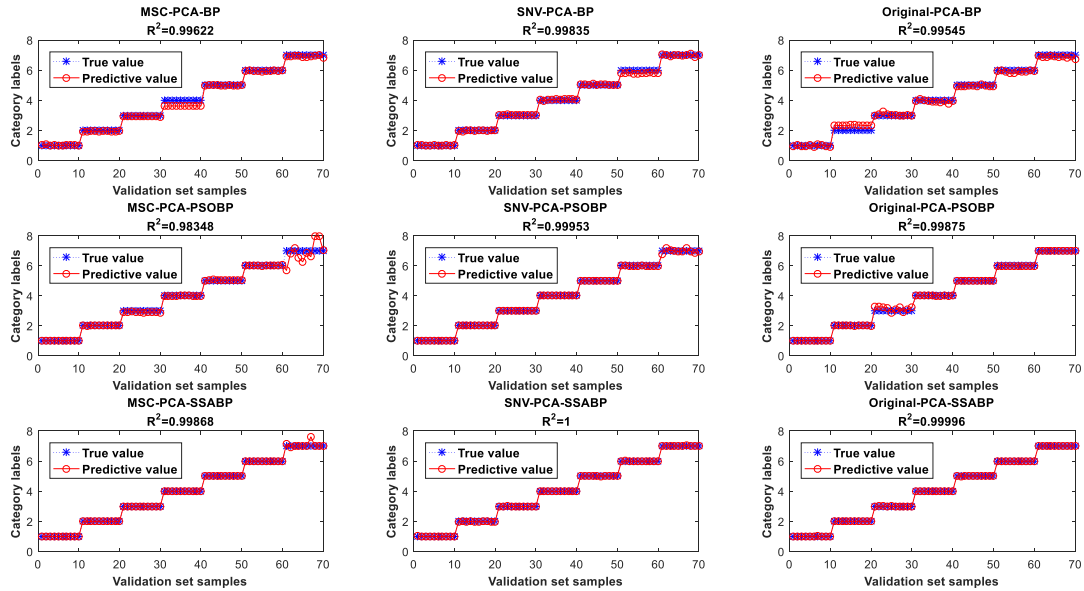


FIGURE 10. Comparison of true values and predictive values of each classification model under different pretreatment methods.

in the above formula, y_i is the true value, f_i is the predicted value, \bar{y} is the average value of the true value.

The mean relative error is the average relative error. The deviation between the predicted value and the true value is obtained by using the absolute error and the true value. The calculation formula of the relative error is as follows.

$$E = \frac{|f_i - y_i|}{y_i} \quad (9)$$

The mean relative error MRE can reflect the deviation between the predicted value and the real value to a large extent [61]. Compared with the relative error, it can reflect the reliability of the prediction better. The calculation formula is as follows.

$$MRE = \sum_i \frac{|f_i - y_i|}{y_i} \quad (10)$$

Root mean square error (RMSE) is a measure of accuracy, also known as standard error. It is used to compare the prediction errors of different models of characteristic data sets [62], [63]. The RMSE value is always non negative, and the lower RMSE is usually better than the higher RMSE. The closer its value is to 0, the more suitable the model is for data processing. The calculation formula is as follows. n is the number of measurements.

$$RMSE = \sqrt{\frac{1}{n} \sum_i (f_i - y_i)^2} \quad (11)$$

The seven proportions of water samples in this experiment were numbered 1–7, and each sample contained 30 sets of experimental data. The first 20 sets of data for each sample were used as the training set for model calculation, and the last 10 sets of data were used as the test set, a total

of 140 sets of training data and 70 sets of test data. After the MSC and SNV pretreatment algorithm, PCA is used to reduce the dimension, and the data after dimension reduction is substituted into each prediction classification model and the predictive value and true value are compared, as shown in Fig. 10. The smallest coefficient of determination is the PSO-BP classification model that uses MSC pretreatment algorithm, and its value is approximately 0.9835. The largest is the SSA-BP classification model with SNV pretreatment, and the coefficient of determination is infinitely close to 1, followed by Original SSA-BP, and the coefficient of determination is 0.9999.

According to the comparison figure, in the BP neural network, the three pretreatments are generally classified, but there is a large deviation in the specific prediction, especially the 30–40 samples in MSC pretreatment, the 50–60 samples in SNV pretreatment, and the 10–20 samples in Original pretreatment. In the PSO-BP classification model, three kinds of pretreatment prediction performance are better, and the types of water samples are basically classified accurately. However, some misjudgments will occur in MSC and SNV pretreatment in samples 60-70, especially the last 10 samples after MSC pretreatment are poor. Original pretreatment will cause obvious misjudgments in samples 20-30. In the SSA-BP classification model, the three pretreatment classification models basically meet the experimental requirements, while the SNV and Original pretreatment have higher accuracy, and the classification results are basically in line with the true values, and they perform well. Therefore, SNV-SSA-BP and Original-SSA-BP have better classification performance in BP, PSO-BP, and SSA-BP classification models under three pretreatment methods. Because the coefficient of determination R^2 of SNV-SSA-BP is 1 and other evaluation indexes

TABLE 2. Comparison of evaluation indexes of different classification models under different pretreatment methods.

Pretreatment	Evaluation Index	BP	PSO-BP	SSA-BP
SNV	R ²	0.9983	0.9995	1
	MRE	0.0140	0.0026	0.0017
	RMSE	0.0075	0.0019	0.0001
MSC	R ²	0.9962	0.9835	0.9987
	MRE	0.0288	0.0197	0.0018
	RMSE	0.0235	0.0669	0.0056
Original	R ²	0.9955	0.9988	0.9999
	MRE	0.0441	0.0091	0.0042
	RMSE	0.0249	0.0054	0.0049

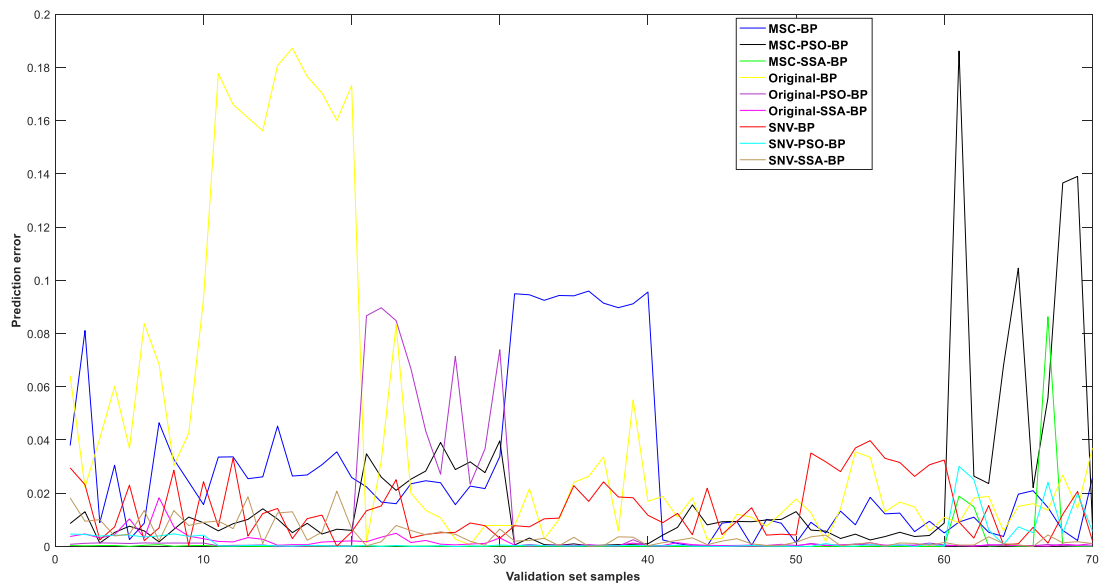


FIGURE 11. Absolute error chart of classification value and true value of each model.

are better than Original-SSA-BP, so SNV-SSA-BP is more suitable for classification and identification of coal mine water sources.

According to the evaluation indexes of each classification model of different pretreatment algorithms in Table 2, the classification model of SNV-SSA-BP algorithm has the best classification effect. The mean relative error MRE is 0.17%, the root mean square error RMSE is 0.01%, and the classification error rate is infinitely close to 0, which can accurately classify and identify mine water sources. The Original-BP model was the worst among the nine classification models in the experiment. The coefficient of determination was 0.9955, the mean relative error (MRE) was 4.41%, and the root mean square error (RMSE) was 2.49%. The difference between Original-BP model and SSA-BP model was close to 4%, and the RMSE was 2%. BP neural network model is preprocessed by SNV, MSC and Original, among which SNV has the best effect. Using PSO and SSA to optimize BP neural network, the classification effect of

SNV-BP classification model algorithm is better than that of PSO-BP classification model, and the classification effect is the best.

As shown in Fig. 11, the absolute error diagrams of BP, PSO-BP and SSA-BP for the predicted and true values of the data after MSC, SNV and Original pretreatment are presented. In the three classification models, the large fluctuation of error amplitude is mainly concentrated in the samples between 10–20, 30–40, 60–70, that is, the prediction classification error of the samples with the number of 2, 4 and 7 changes greatly, and the error amplitude of Original-BP is far greater than that of other prediction models. The maximum absolute error of this model is 0.1872, and the minimum is 0.0006. The minimum absolute error model is SNV-SSA-BP classification model. The maximum absolute error of classification is 0.0208, and the minimum is close to 0.

Under the SNV pretreatment method, the optimal individual fitness value of SSA-BP prediction classification model

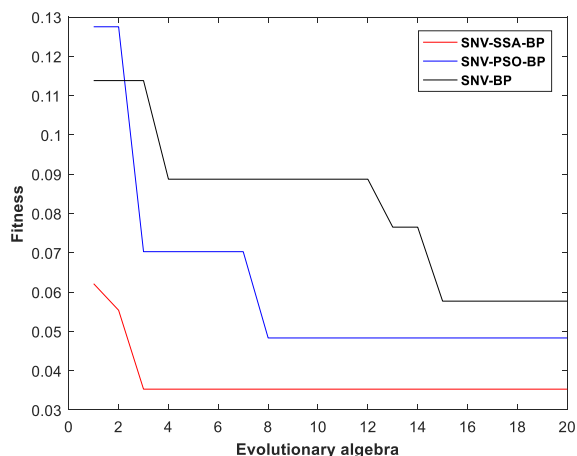


FIGURE 12. The fitness curve.

is 0.0353, which is better than that of PSO-BP and BP model of 0.0483 and 0.0577.

According to the fitness curve, the fitness value of SSA-BP in the whole iteration process of the three prediction classification models is less than that of the other two classification models, and when the number of iterations is 3, it reaches the minimum value of the fitness value and tends to be stable, the convergence effect is the best and the stability is good, while the other two models reach the minimum value of their fitness values respectively when the number of iterations is 8 and 15, and the classification effect is poor. Since the optimal value obtained by SSA-BP algorithm is close to the actual optimal value of the function, and according to the rating factors including MRE, RMSE, and absolute error, the results of SSA-BP prediction classification model are closer to the true value, so the classification ability of the model is better than that of the other two models.

In summary, from the comparison of the classification value and the true value and the analysis of the error results of each model, it can be seen that the classification ability of BP neural network without any pretreatment is the worst. The classification value of SSA-BP is closer to the true value, and the classification performance is better. Therefore, in the prediction and classification model of water source types, SSA-BP is superior to PSO-BP and BP neural network, while PSO-BP neural network classification model is superior to BP neural network.

VI. DISCUSSION

In the safety production of coal mines, mine water inrush is one of the most destructive coal mine accidents, and the source of water inrush generally is goaf water or other groundwater. In this experiment, the experimental material is selected karst water, old goaf water, and the mixing ratio of two water samples as the research object. The original spectral information of water samples is obtained by laser-induced fluorescence device, and it is pretreated by SNV, MSC, and Original. Due to the large amount of data calculation after preprocessing, PCA algorithm is used to reduce the dimension of data, and the data after dimension reduction is

obtained. The spectral data of different types of water samples are numbered 1-7, a total of 210 groups of data, and they are divided into training set and test set. Different classification prediction models are used to compare evaluation indexes, and finally the optimal model identification of mine water source is realized.

Experiments show that the SNV algorithm performs well in the three preprocessing methods of SNV, MSC, and Original, and improves the correlation of the model. Under the premise of SNV pretreatment, the coefficient of determination R^2 of BP was 0.9983, the MRE was 1.4%, and the RMSE was 0.75%. The coefficient of determination R^2 of PSO-BP is 0.9995, the average relative error MRE is 0.26%, and the RMSE is 0.19%. The coefficient of determination R^2 of SSA-BP is infinitely close to 1, the MRE is 0.17%, and the RMSE is 0.01%. For BP, PSO-BP, and SSA-BP algorithm classification model, SNV was selected as the most suitable for prediction classification of seven water samples in three pretreatment methods of SNV, MSC, and Original. Combined with PCA dimension reduction, it was found that SNV-SSA-BP classification performance was the best by comparing different classification models under the same pretreatment method. In this experiment, SNV pretreatment eliminates the influence of scattering and diffuse reflection caused by the unevenness of the sample to be measured in the acquisition of spectrum, and reduces the interference of noise. Reduce dimension by PCA, remove redundant information and reduce computation. The optimal number of hidden layer nodes is selected in BP neural network, and the type number of mine water source is obtained by processing the training set data and applying it to the test set samples. In the PSO algorithm model, the optimal weights and thresholds are given to BP neural network for optimization. Sparrow search algorithm uses the position update of the participants and predators to obtain the optimal fitness and realize the recognition and classification of mine water inrush.

VII. CONCLUSION AND PROSPECT

A. BP NEURAL NETWORK

In this experiment, the LIF technology is proposed to identify the water source of coal mines, which provides a new solution for the subsequent mine water inrush accidents. The algorithm used is optimized on the basis of the BP neural network algorithm. The combination of laser-induced fluorescence and neural network algorithm is a targeted innovation in the field of mine water source identification.

In this experiment, the fluorescence spectra of different proportions of mixed water inrush samples were collected, and a database of mine water sources was established. On this basis, the identification models of different prediction classifications are established, and the data of coal mine water sources are combined with the identification model to classify the coal mine water sources. The experimental object is karst water, old goaf water, and the mixture ratio of the two water samples which were collected from Xinzhuanzi coal mine, classification model uses BP neural network algorithm to

classify samples. The experimental results and conclusions are as follows:

- 1) The important position of coal mining in national economic development and the significant harm of mine water disasters to coal mining are introduced in detail.
- 2) The types and causes of water inrush are studied, which provides background significance for the classification of mine water sources in the later period.
- 3) This experiment expounds the development status and application fields of LIF technology, and introduces the simple steps of using LIF technology to identify coal mine water source.
- 4) The laser-induced fluorescence experimental device is briefly introduced, including laser emitter, spectrometer and fluorescence probe.
- 5) The acquisition process of spectral data of coal mine water source is described in detail. At the same time, the simple spectral pretreatment of the original data is carried out.
- 6) PCA dimensionality reduction is performed on the pre-processed data, and the main purpose is to reduce the computational complexity by noise reduction, so that it can better adapt to the model processing.
- 7) The classification model of coal mine water source is established, the BP neural network and its optimization algorithm are briefly described. According to the characteristics of different optimization algorithms, the classification of coal mine water source is judged.
- 8) The collected coal mine water sources were classified and optimized by different BP optimization algorithms, and the model was well compared according to the classification results.

B. PROSPECT

For the increasingly serious problem of coal mine water inrush, this experiment puts forward the use of laser induced fluorescence technology to identify coal mine water source, which can provide technical support for the prevention and control of coal mine water inrush in the future. However, due to the complexity of the research problem, the workload of the experiment and the limitation of cognitive level, there are still many deficiencies in this experimental study, and many unin-depth problems have not been satisfactorily solved, which need further efforts in the following aspects:

The experimental object is only two kinds of water inrush samples and mixed water samples with different proportions. The identification model of coal mine water inrush based on LIF technology requires a large number of representative coal aquifer water samples as the research basis, so as to obtain more comprehensive water inrush data, and the model processing results can be more reliable and persuasive. Therefore, in the subsequent experiments should not only increase the types of water inrush samples, but also continue to expand the study of coal mine area, improve the model database.

This experiment is carried out under laboratory conditions, and the audit and detection of equipment are more stringent

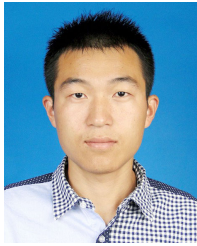
in the practical application of underground. Whether from the portability or safety of equipment, it will continue to explore and study in the subsequent work.

In the experiment, when the LIF technology is used to obtain the fluorescence spectrum of water inrush samples, the water inrush samples are standing on the experimental table. However, when the actual spectrum is collected, the water inrush in coal mines has a certain flow rate. Therefore, in the subsequent studies, the influence of the flow of water inrush on the fluorescence signal will be eliminated to achieve accurate and stable acquisition of fluorescence spectrum.

REFERENCES

- [1] H. Huang, "Research on commodity property of coal under market economy," *China Coal*, vol. 47, no. 1, pp. 52–56, Jan. 2021.
- [2] H.-P. Xie, L.-X. Wu, and D.-Z. Zheng, "Prediction on the energy consumption and coal demand of China in 2025," *J. China Coal Soc.*, vol. 44, no. 7, pp. 1949–1960, Jul. 2019.
- [3] L.-F. Zhu and X. Y. Zhu, "Economic prying effect of de-capacity and asset structure adjustment in the coal industry," *Resour. Sci.*, vol. 43, no. 2, pp. 316–327, Feb. 2021.
- [4] L. Xiao, "Decoupling analysis between coal consumption and economic growth in Beijing-Tianjin-Hebei Region," *Coal Eng.*, vol. 52, no. 9, pp. 188–192, Sep. 2020.
- [5] X.-M. Sun, "Research and practice on high quality development strategy of coal industry," *Coal Eng.*, vol. 51, no. 1, pp. 152–156, Jan. 2019.
- [6] X.-B. Song, T. Yang, and X.-F. Song, "Research on high quality development strategy of coal industry in new era," *Coal Eng.*, vol. 50, no. 12, pp. 163–167, Dec. 2018.
- [7] A.-G. Zhao and Z.-X. Li, "Contribution of the coal industry to China's national economy," *J. Liaoning Tech. Univ.*, vol. 33, no. 5, pp. 716–720, May 2014.
- [8] M. Dzikuc, P. Kurylo, R. Dudziak, S. Szufa, M. Dzikuc, and K. Godzisz, "Selected aspects of combustion optimization of coal in power plants," *Energies*, vol. 13, no. 9, pp. 1–15, May 2020.
- [9] I. Jonek-Kowalska, "Consolidation as a risk management method in the lifecycle of a mining company: A novel methodological approach and evidence from the coal industry in Poland," *Resour. Policy*, vol. 60, pp. 169–177, Mar. 2019.
- [10] C. Mark and G. M. Rumbaugh, "Assessing risks from mining-induced ground movements near gas wells," *Int. J. Mining Sci. Technol.*, vol. 30, no. 1, pp. 11–16, Jan. 2020.
- [11] B. C. Olsen, K. Awuah-Offei, and D. Bumblauskas, "Setting materiality thresholds for ESG disclosures: A case study of U. S. mine safety disclosures," *Resour. Policy*, vol. 70, Mar. 2021, Art. no. 101914.
- [12] I. M. Jiskani, B. Ullah, K. S. Shah, S. Bacha, N. M. Shahani, M. Ali, A. Maqbool, and A. R. Qureshi, "Overcoming mine safety crisis in Pakistan: An appraisal," *Process Saf. Prog.*, vol. 38, no. 4, Dec. 2019.
- [13] K. Doss, A. S. Hanshew, and J. C. Mauro, "Signatures of criticality in mining accidents and recurrent neural network forecasting model," *Phys. A, Stat. Mech. Appl.*, vol. 537, Jan. 2020, Art. no. 122656.
- [14] E. Atay and J. L. Y. Terpstra-Tong, "The determinants of corporate social irresponsibility: A case study of the soma mine accident in Turkey," *Social Responsibility J.*, vol. 16, no. 8, pp. 1433–1452, Nov. 2019.
- [15] S. Şalap, M. O. Karslıoğlu, N. Demirel, "Development of a GIS-based monitoring and management system for underground coal mining safety," *Int. J. Coal Geol.*, vol. 80, no. 2, pp. 105–112, Nov. 2009.
- [16] S. Dong, X. Guo, Q. Liu, H. Wang, and S. Nan, "Model and selection criterion of zonal preact grouting to prevent mine water disasters of coal floor limestone aquifer in North China type coalfield," *Coal Geol. Explor.*, vol. 48, no. 4, pp. 1–10, Aug. 2020.
- [17] P.-D. Guan and Y. Li, "Influencing factors and relationship analysis of mechanical and electrical accidents in mine," *Coal Chem. Ind.*, vol. 41, no. 5, pp. 66–68, May 2018.
- [18] W. Yang, G. Fu, J. Y. Dong, W. Yin, N. Shao, S. Qing, and K. Zhu, "Analysis and solutions of unsafe act in the coal mine blasting accidents," *Saf. Coal Mines*, vol. 44, no. 6, pp. 230–232, Jun. 2013.
- [19] X.-L. Ning, "Law analysis and counter measures research of coal mine accidents in China from 2013 to 2018," *Ind. Mine Autom.*, vol. 46, no. 7, pp. 34–41, Jul. 2020.

- [20] J.-P. Lu, Y.-D. Li, J.-H. Wu, J. Zhao, and H.-L. Bai, "Study of collaborative emergency problems based on fire fighting forces," *Fire Sci. Technol.*, vol. 37, no. 12, pp. 1742–1746, Dec. 2018.
- [21] B. Li, Q. Wu, and Z. Liu, "Identification of mine water inrush source based on PCA-FDA: Xiandewang coal mine case," *Geofluids*, vol. 2020, pp. 1–8, Aug. 2020.
- [22] M. M. R. Sarker, M. Van Camp, D. Hossain, M. Islam, N. Ahmed, M. M. Karim, M. A. Q. Bhuiyan, and K. Walraevens, "Groundwater salinization and freshening processes in coastal aquifers from southwest Bangladesh," *Sci. Total Environ.*, vol. 779, Jul. 2021, Art. no. 146339.
- [23] H. Achyuthan, R. D. Deshpande, M. S. Rao, B. Kumar, T. Nallathambi, K. Shashi Kumar, R. Ramesh, P. Ramachandran, A. S. Maurya, and S. K. Gupta, "Stable isotopes and salinity in the surface waters of the bay of bengal: Implications for water dynamics and palaeoclimate," *Mar. Chem.*, vol. 149, pp. 51–62, Feb. 2013.
- [24] B. Kumar, S. P. Rai, U. S. Kumar, S. K. Verma, P. Garg, S. V. V. Kumar, R. Jaiswal, B. K. Purendra, S. R. Kumar, and N. G. Pande, "Isotopic characteristics of Indian precipitation," *Water Resour. Res.*, vol. 46, no. 12, Dec. 2010.
- [25] M. A. Allison, S. R. Khan, S. L. Goodbred, and S. A. Kuehl, "Stratigraphic evolution of the late Holocene Ganges–Brahmaputra lower delta plain," *Sedimentary Geol.*, vol. 155, nos. 3–4, pp. 317–342, Feb. 2003.
- [26] S.-J. Chen, "Technological research on water source identification of coastal coalmines based on PCA-RA," *Coal Sci. Technol.*, vol. 49, no. 2, pp. 217–225, Feb. 2020.
- [27] Y.-Q. Jin, J.-H. Long, J. Ren, and X.-L. Ni, "Water source analysis of mine filling foundation based on hydrochemical characteristics," *Coal Science and Technology*, to be published. [Online]. Available: <http://kns.cnki.net/kcms/detail/11.2402.TD.20200803.1815.002.html>
- [28] Z.-H. Jiang, Y.-B. Hu, Q.-D. Ju, L. Zhou, and S.-Y. Shu, "A discrimination method of mine water inrush source," *Ind. Mine Autom.*, vol. 46, no. 4, pp. 28–33, Apr. 2020.
- [29] J.-K. Xue, "Quantitative analysis of mine water inrush using isotope method," *Coal Eng.*, vol. 51, no. 12, pp. 150–153, Dec. 2019.
- [30] L.-Q. Shi, X.-L. Wang, M. Qiu, and W.-F. Gao, "Recognition of limestone water inrush source by Fisher method of traceelements," *China Sci.*, vol. 15, no. 5, pp. 491–496, May 2020.
- [31] D.-S. Zhang, W. Zhang, L.-Q. Ma, X.-F. Wang, and G.-W. Fan, "Developments and prospects of detecting mining-induced fractures in overlying strata by radon," *J. China Univ. Mining Technol.*, vol. 45, no. 6, pp. 1082–1097, Nov. 2016.
- [32] L. Ma, J.-Z. Qian, and W.-D. Zhao, "An approach for quickly identifying water-inrush source of mine based on GIS and groundwater chemistry and temperature," *Coal Geol. Explor.*, vol. 42, no. 2, pp. 49–53, Apr. 2014.
- [33] W.-J. Li, X.-Y. Zhang, F.-L. Li, and Z.-Y. Li, "Water inrush prediction and information management system based on GIS technology," *Saf. Coal Mines*, vol. 47, no. 3, pp. 107–110, Mar. 2016.
- [34] W.-T. Wang, M. Zhang, S. Zhao, and Z. Liu, "Application of laser-induced fluorescence technique in visualization of liquid mixing process," *CIESC J.*, vol. 64, no. 3, pp. 771–778, Mar. 2013.
- [35] T. Li, S.-Y. Chen, Y.-C. Zhang, P. Guo, H. Chen, and Y. Li, "Quantification of adulterated extra virgin olive oil using laser induced fluorescence," *Spectrosc. Spectral Anal.*, vol. 38, no. 10, pp. 285–286, Oct. 2018.
- [36] Z.-L. Zuo, Z. Nan-Jing, M. De-Shuo, H. Yao, Y. Gao-Fang, and L. Jian-Guo, "Study on the overlapping characteristics of fluorescence signals of machine oil and diesel mixtures in soil based on iterative approximation algorithm," *Spectrosc. Spectral Anal.*, vol. 40, no. 1, pp. 310–315, Jan. 2020.
- [37] G. G. Wang, S. Deb, and Z. Cui, "Monarch butterfly optimization," *Neural Comput. Appl.*, vol. 31, no. 7, pp. 1995–2014, 2019.
- [38] S. Li, H. Chen, M. Wang, A. A. Heidari, and S. Mirjalili, "Slime mould algorithm: A new method for stochastic optimization," *Future Gener. Comput. Syst.*, vol. 111, pp. 300–323, Oct. 2020.
- [39] G.-G. Wang, "Moth search algorithm: A bio-inspired metaheuristic algorithm for global optimization problems," *Memetic Comput.*, vol. 10, pp. 151–164, Jun. 2018.
- [40] Y. Yang, H. Chen, A. A. Heidari, and A. H. Gandomi, "Hunger games search: Visions, conception, implementation, deep analysis, perspectives, and towards performance shifts," *Expert Syst. Appl.*, vol. 177, Sep. 2021, Art. no. 114864.
- [41] I. Ahmadianfar, A. A. Heidari, A. H. Gandomi, X. Chu, and H. Chen, "RUN beyond the metaphor: An efficient optimization algorithm based on Runge Kutta method," *Expert Syst. Appl.*, vol. 181, Nov. 2021, Art. no. 115079.
- [42] A. A. Heidari, S. Mirjalili, H. Faris, I. Aljarah, M. Mafarja, and H. Chen, "Harris hawks optimization: Algorithm and applications," *Future Gener. Comput. Syst.*, vol. 97, pp. 849–872, Aug. 2019.
- [43] L.-Q. Luo, X.-L. Yao, and S.-L. He, "Study on the method of determining the survival rate of rice seeds based on visible-near infrared multispectral data," *Spectrosc. Spectral Anal.*, vol. 40, no. 1, pp. 221–226, Jan. 2020.
- [44] W.-L. Qiu, Y.-W. Zhou, and M.-L. Shi, "Classification of vehicle bumpers through micro-laser Raman spectroscopy based on PCA-LDA," *China Plastics*, vol. 35, no. 1, pp. 78–83, Jan. 2021.
- [45] Y. Du, X.-C. Meng, and L.-Q. Zhu, "Overlapping spectral analysis based on genetic algorithms and BP neural networks," *Spectrosc. Spectral Anal.*, vol. 40, no. 7, pp. 2066–2072, Jul. 2020.
- [46] H.-S. Song, L.-Z. Ma, E.-G. Zhu, Y.-F. Wang, Y.-P. Liu, W.-J. Sun, P. Peng, and C.-F. Li, "Plastic classification and recognition by laser-induced breakdown spectroscopy and GA-BP neural network," *Laser Optoelectron. Prog.*, vol. 57, no. 15, pp. 262–269, Aug. 2020.
- [47] Z. Zheng, S. Dai, and X. Xie, "Research on fault detection for ZPW-2000A jointless track circuit based on deep belief network optimized by improved particle swarm optimization algorithm," *IEEE Access*, vol. 8, pp. 175981–175997, 2020.
- [48] B.-Z. Huang, J.-H. Yang, S.-L. Lu, H.-F. Chen, and D.-S. Xie, "Wave capture power forecasting based on improved particle swarm optimization neural network algorithm," *Acta Energetica Solaris Sinica*, vol. 42, no. 2, pp. 302–308, Feb. 2021.
- [49] Q. Feng, Q. Li, W. Quan, and X.-M. Pei, "Overview of multiobjective particle swarm optimization algorithm," *Chin. J. Eng.*, vol. 43, pp. 745–753, Jun. 2021.
- [50] T.-X. Wen, X. Sun, X.-B. Kong, and H.-B. Tian, "Research on prediction of gas emission quantity with sub sources basing on PSOBP-AdaBoost," *China Saf. Sci. J.*, vol. 26, no. 5, pp. 94–98, May 2016.
- [51] C.-J. Deng, B. Ouyang, and Y.-H. Chen, "A building settlement prediction model based on PSO-BP neural network," *Sci. Surv. Mapping*, vol. 43, no. 6, pp. 27–31+38, Jun. 2018.
- [52] L. Wang, R.-Y. Hao, W. Liu, and Z.-M. Wen, "A multi-factor forest fire risk rating prediction model based on particle swarm optimization algorithm and back-propagation neural network," *J. Forestry Eng.*, vol. 4, no. 3, pp. 137–144, 2019.
- [53] C. Zhou, H.-B. Gao, L. Gao, and W.-G. Zhang, "Particle swarm optimization(PSO) algorithm," *Appl. Res. Comput.*, vol. 12, pp. 7–11, Oct. 2003.
- [54] X. Lv, X.-D. Mu, J.-Zhang, and Z. Wang, "Chaos sparrow search optimization algorithm," *J. Beijing Univ. Aeronaut. Astronaut.*, to be published. [Online]. Available: <https://kns.cnki.net/kcms/detail/detail.aspx?doi=10.13700/j.bh.1001-5965.2020.0298>
- [55] C.-T. Shi, Y.-Y. Zeng, and S.-M. Hou, "Summary of the application of swarm intelligence algorithms in image segmentation," *Comput. Eng. Appl.*, vol. 57, no. 8, pp. 36–47, Aug. 2021.
- [56] C. Ouyang, Y. Qiu, and D. Zhu, "A multi-strategy improved sparrow search algorithm," *J. Phys., Conf. Ser.*, vol. 1848, no. 1, Apr. 2021, Art. no. 012042.
- [57] X. Lv, X.-D. Mu, and J. Zhang, "Multi-threshold image segmentation based on improved sparrow search algorithm," *Syst. Eng. Electron.*, vol. 43, no. 2, pp. 318–327, Feb. 2021.
- [58] A.-D. Tang, T. Han, D.-W. Xu, and L. Xie, "Path planning method of unmanned aerial vehicle based on chaos sparrow search algorithm," *J. Comput. Appl.*, vol. 41, no. 7, pp. 2128–2136, Jul. 2021.
- [59] Y.-Y. Hu, S.-J. Wang, and S.-G. Chen, "Research on prediction methods of sloping breakwater overtopping based on machine learning," *Sci. Technol. Ind.*, vol. 21, no. 2, pp. 218–224, Feb. 2021.
- [60] S.-L. Tian, T. Chen, M.-N. Tang, and L. Yang, "Research on data duplicates-removing method based on coefficient of relevance and coefficient of determination," *Digit. Manuf. Sci.*, vol. 17, no. 3, pp. 241–244, Sep. 2019.
- [61] X.-X. Qin, W.-B. Liu, and L.-C. Chen, "Pipeline corrosion prediction based on an improved artificial bee colony algorithm and a grey model," *J. Beijing Univ. Chem. Technol.*, vol. 48, no. 1, pp. 74–80, Jan. 2021.
- [62] H.-Z. Xue, C.-J. Wang, H.-M. Zhou, J.-D. Wang, and H.-W. Wan, "BP neural network based on simulated annealing algorithm for high resolution LAI retrieval," *Remote Sens. Technol. Appl.*, vol. 35, no. 5, pp. 1057–1069, Oct. 2020.
- [63] X.-W. Chen, W.-Y. Zhu, X.-M. Qian, T. Luo, G. Sun, Q. Liu, X.-B. Li, and N.-Q. Weng, "Estimation of surface layer optical turbulence using artificial neural network," *Acta Optica Sinica*, vol. 40, no. 24, pp. 15–21, Dec. 2020.



PENGCHENG YAN received the B.E., M.E., and Ph.D. degrees from Anhui University of Science and Technology, Huainan, China. He is currently a Postdoctoral Researcher and a Lecturer with Anhui University of Science and Technology. His current research interests include laser information processing and in-depth research on spectral analysis techniques.



XIAOFEI ZHANG received the B.E. degree in automation specialty from Anhui University of Science and Technology, Huainan, China, in 2020, where he is currently pursuing the M.E. degree in control science and engineering. His research interests include data analysis and digital picture processing technique.



SONGHANG SHANG received the B.E. degree in communication engineering from the City Institute, Dalian University of Technology, Dalian, China, in 2018. He is currently pursuing the M.E. degree with Anhui University of Science and Technology, Huainan, China. His current research interests include pattern recognition and spectral analysis technology.



GAOKUN YANG received the B.E. degree in building electrical and intelligent from Guangling College, Yangzhou University, Yangzhou, China, in 2019. He is currently pursuing the M.E. degree in electrical engineering with Anhui University of Science and Technology, Huainan, China. His current research interests include deep learning and image processing.



CHAOYIN ZHANG received the B.E. degree in electrical engineering and automation from Chaohu College. He is currently pursuing the M.E. degree in energy dynamics with Anhui University of Technology, focusing on data analysis and photoelectric information processing.



ZHUANG ZHANG received the B.E. degree in electrical power engineering from Changchun University of Architecture. He is currently pursuing the M.E. degree in electrical engineering with Anhui University of Science and Technology. His research interest includes deep learning. He is very interested in all kinds of algorithms and making continuous efforts in this direction.



NINI YIN received the M.E. degree in engineering management from Anhui University of Science and Technology. Her current research interests include deep learning and in-depth research on data analysis.



QUANSHENG SUN is currently pursuing the B.E. degree with Anhui University of Science and Technology. His research interests include machine vision, image processing, and machine learning.

...